J Nanopart Res (2013) 15:1418
DOI 10.1007/s11051-013-1418-7

RESEARCH PAPER

Persistence of commercial nanoscaled zero-valent iron (nZVI) and by-products

Adeyemi S. Adeleye · Arturo A. Keller · Robert J. Miller · Hunter S. Lenihan

Received: 7 June 2012 / Accepted: 5 January 2013 / Published online: 18 January 2013

Abstract The use of nanoscale zero-valent iron (nZVI) for in situ remediation of a wide scale of environmental pollutants is increasing. Bench and field pilot studies have recorded successful cleanup of many pollutants using nZVI and other iron-mediated nanoparticles. However, a major question remains unanswered: what is the long-term environmental fate of the iron nanoparticles used for remediation? We aged three types of commercial nZVI in different aqueous media, including a groundwater sample, under aerobic and anaerobic conditions for 28 days, and found that the bulk of the nZVI injected into polluted sites will end up in the sediment phase of the aquifer. This is mainly due to aggregation-induced sedimentation of the nZVI and the insoluble iron oxides formed when nZVI undergoes corrosion. Iron concentrations >500 g/kg were detected in sediment, a loading level of iron that may potentially affect some organisms and also reduce the permeability of aquifers. Dissolved and suspended iron concentrations initially surged when nZVI was applied, but iron decreased steadily in the supernatant and suspended sediment as the bulk of the iron partitioned into the sediment. Solution and surface chemistry of the iron species showed that nZVI remains reactive for more than 1 month, and that the reactivity of iron and its transformations are governed by environmental factors, including the presence of different ions, ionic strength, natural organic matter, and pH.

Keywords Nanoscaled zero-valent iron (nZVI) · Iron oxide · Persistence · Fate and transport · In situ remediation · Nanoremediation · Environmental implication

Introduction

The goal of environmental remediation is to remove or control pollutants in soil, sediments, groundwater, and surface water to reduce the human and ecological risk posed by hazardous waste sites (Karn et al. 2009; Holland 2011). Pollutants and their sources are diverse in nature, and consequently several remediation methods have emerged over the years (Francis and Dodge 1998; Kirchner et al. 2011; Rodgers and Bunce 2001). Remedial actions are frequently energy intensive and expensive and can also produce their own contaminations and impacts (Karn et al. 2009; Holland 2011). As a result, practitioners seek more environmentally, socially, and economically sustainable methods for pollution cleanup (Holland 2011).

Electronic supplementary material The online version of this article (doi:10.1007/s11051-013-1418-7) contains supplementary material, which is available to authorized users.

A. S. Adeleye · A. A. Keller (✉) · R. J. Miller · H. S. Lenihan
Bren School of Environmental Science & Management, University of California, Santa Barbara, 3420 Bren Hall, Santa Barbara, CA 93106-5131, USA
e-mail: keller@bren.ucsb.edu

Nanoremediation has recently emerged as a cleanup method that appears to reduce costs, improve effectiveness, and generate fewer hazardous by-products (Karn et al. 2009; Simon 1997; Xi et al. 2011; Zhang 2003; Crane and Scott 2012).

Nanoremediation, the use of nanomaterials for environmental pollutants cleanup, is based on the ability of certain nanomaterials to either react with the pollutant of concern or create an enabling environment for its transformation into less toxic or nontoxic forms (Karn et al. 2009; Ponder et al. 2000; O'Carroll et al. 2012; Mueller et al. 2012; Pan and Xing 2012). Nanoremediation can also occur via adsorption of the pollutants (e.g., heavy metals) to the nanoparticles, thereby immobilizing them (Ponder et al. 2000; Theron et al. 2008; Tratnyek and Johnson 2006; Zhang 2003). For many problematic pollutants, such as chlorinated organic compounds, nanoremediation may be a viable, efficient, and cost effective alternative to traditional in situ remediation technologies, such as pump-and-treat, chemical oxidation, and bioremediation (Karn et al. 2009; Otto et al. 2008). Relative to more conventional methods, nanoremediation also has the potential to decrease the overall remediation timeframe, due to the higher reactivity of nanomaterials, and can eliminate the need for treatment and disposal of contaminated soil since it can be applied in situ (Karn et al. 2009; Zhang 2003). In particular, nanoscale zero-valent iron (nZVI) has been proposed or applied for the remediation of a wide array of common environmental contaminants such as chlorinated organic solvents (Amir and Lee 2011; Li et al. 2006; Tee et al. 2009; Zhang et al. 2011; Zhang and Elliott 2006; Wei et al. 2012), organochlorine pesticides (Joo and Zhao 2008; Zhang and Elliott 2006), polychlorinated biphenyls (He and Zhao 2005), organic dyes (Fan et al. 2009; Xi et al. 2011), and heavy metals such as arsenic, mercury, zinc, lead, and chromium ions (Kanel et al. 2006; Ponder et al. 2000; Zhang and Elliott 2006; Yan et al. 2010; Yan et al. 2012). The use of nZVI to remediate pollutants has gained increasing attention in recent years, primarily due of its wide application options, high degree of reactivity (Chang and Kang 2009; Karn et al. 2009; Grieger et al. 2010) and perceived environmentally benign characteristics (Xi et al. 2011; Zhang 2003).

While many studies have shown the effectiveness of nZVI in pollution remediation, only a few studies have investigated the potential impact the use of this technology may have on the both the physical environment and the biological systems at the point of application and its surroundings (Sun et al. 2006, 2007; Zhang and Elliott 2006). Studies have shown that nZVI and its oxide can have toxic effects on a variety of life forms (Auffan et al. 2008; Keller et al. 2012; Chen et al. 2011b; Wang et al. 2011). As such, it is essential to understand the nature and rate of transformation that occur to nZVI particles and the environment into which they are applied. In addition, the surface and chemical properties of nZVI change significantly over time with solution chemistry and environmental conditions (Li et al. 2006). This implies that their effect on the environment and the ecosystem may also change with time. The aggregation and sedimentation rates of different concentrations of nZVI have been monitored on a short term basis (within a few hours) (Phenrat et al. 2007). However, there has been no long-term study of nZVI aggregation and how nZVI and its oxidation products may partition between the supernatant and sediment phases when injected into the aquifer. Also, there is currently almost no data on the potential persistency of nZVI and its transformation products (Grieger et al. 2010).

Thus, the objective of this study was to (1) investigate the persistence of different types of nZVI aged in different aqueous media, and observe the partitioning of the iron species into the various phases of the aqueous media, (2) monitor nZVI transformation (change in surface chemistry) and solution chemistry as the nZVI ages, and (3) investigate how aquifer properties such as ionic strength affect these transformations.

Experimental

Aqueous suspensions of three types of commercial nZVI, Nanofer STAR (NS), Nanofer 25S (N25S), and Nanofer 25SS (N25SS) were prepared in NanoPure water (Barnstead), 10 mM $CaCl_2$, 100 mM $CaCl_2$, and a groundwater sample (RW) obtained from a remediation well of a polluted site. Characterization of RW is shown in Table S3 (Online Resource 1). All the nZVI samples were obtained from NANO IRON (Czech Republic) and preserved in a 4 °C constant-temperature room before the experiment. NS is an air-stable nZVI powder, consisting of Fe^0 surface stabilized nanoparticles. N25S is an aqueous dispersion of nZVI coated with

polyethylene glycol sorbitan monostearate, a surfactant. N25SS was received as an aqueous dispersion of NS, which was further treated by shear-mixing. Iron oxides shells are usually formed on exposure of the Fe^0 to aqueous media or air (Sun et al. 2006; Yan et al. 2010). The primary nZVI particles are 20–100 nm in diameter, with surface area of 20–25 m^2/g, and a particle density of 1,150–1,250 kg/m^3, as reported by the manufacturer. The three nZVI samples were characterized by nanoparticles tracking analysis (NTA, NanoSight LM10-HS) and X-ray diffraction (XRD, Bruker D8 Advance). The XRD scans were evaluated using Bruker DIFFRAC^{plus} EVA software. For the NTA measurements, 100 mg/L stock suspension of each nZVI was sonicated in a water bath (Branson 1310, Danbury, CT) for 30 min. The stock was then diluted to 10 mg/L using nitrogen-purged NanoPure water and the pH was adjusted to 7.0 with phosphate buffer (Fisher Scientific) before measurement. Scanning electron microscopy (SEM, FEI XL30 Sirion) and BET surface area analysis (Micromeritics TriStar 3000 porosimeter) of NS dry powder were also done. SEM and BET surface area analysis were not done for N25S and N25SS because they were received in aqueous form and drying them for the analyses would substantially alter their morphology.

We prepared a fresh aqueous suspension of NS just before this study while N25S and N25SS stocks were diluted to the desired concentration—as would be done in an in situ remediation project (Zhang and Elliott 2006). Each suspension had a volume of 500 mL with nZVI concentration of 3 g/L (except for two RW controls). nZVI concentrations commonly used for pollution remediation are 1–30 g/L (Li et al. 2006; Sun et al. 2007; Zhang 2003; Jiemvarangkul et al. 2011; Mueller et al. 2012; Wei et al. 2012).

Two sets of each nZVI were suspended in each aqueous media—one set for aerobic and another for anaerobic conditions. Each suspension was sonicated at 40 amps for 1.5 min with a Misonix Sonicator S-4000 (QSonica LLC, Newtown, CT) and then adjusted to ~pH 7.0 using 0.1 M NaOH and HCl. The pH of the RW suspensions was not adjusted. From each of the 500 mL suspensions, seven 30 mL aliquots were made and kept in the same condition as the original stock. These 30 mL aliquots were sampled sequentially (Days 0, 1, 2, 4, 7, 14, and 28) to monitor the chemistry of each condition. The original larger stock suspensions remained undisturbed and were used to monitor the partitioning of iron species between the supernatant and the sediment phases. The experiments were conducted under well-aerated conditions for the aerobic experiment, and with an ultra-high grade nitrogen gas blanket within a glove box for the anaerobic conditions.

Total iron concentrations ($[Fe]_{total}$) were analyzed via ICP-AES (iCAP 6300, Thermo Scientific) using the Fe2395 line. NIST-traceable standard solutions for iron (Fluka Analytical) were used to generate calibration curves ranging from 0.05 to 100 mg/L. Zeta (ζ) potential, hydrodynamic size, count rate, and conductivity of the nZVI suspensions were monitored with a Zetasizer Nano-ZS90 (Malvern, UK) using folded capillary cells. Each data point obtained with the Zetasizer was an average of three repetitions of 10 or more runs each. Sample pH and oxidation–reduction potential (ORP) were monitored with HACH HQ 40d portable meter. Temperature was monitored using a Dual Thermometer TYPE K (Fisher Scientific). To determine $[Fe]_{total}$ in the sediment, a known mass of sediment from a given sample was digested in 5 mL nitric acid at 80 °C for 60 min in a Precision Reciprocal Shaking bath (Thermo Scientific). The digested sample was then poured into a 50 mL volumetric flask and the volume was made up with NanoPure water. 10 mL of the diluted samples were then analyzed via ICP-AES and the result corrected for the dilutions. To determine the total iron concentration in the supernatant phase, 3 mL of the samples' supernatant was carefully pipetted into 10 K Amicon® Ultra-4 centrifugal filter tubes (Millipore, Ireland) and centrifuged at 8,000 rpm for 20 min (RC 5B Plus, Sorvall, Newtown, CT). 1 mL of the filtrate was digested in 1 mL of nitric acid and then diluted with 8 mL NanoPure water before ICP-AES analysis. The filtrand, collected in the filter unit of the Amicon® tubes, was also digested and analyzed via ICP-AES to determine $[Fe]_{total}$ in the suspended sediment phase. To determine the ferrous ion concentration in the supernatant, 250 µL of sample was diluted in 24.75 mL of nitrogen-purged NanoPure water and then analyzed with a HACH DR/890 Colorimeter, using HACH Ferrous iron reagent powder pillows.

Results and discussion

nZVI characterization

The NTA analysis showed that the nZVI particles are polydispersed, with the highest polydispersity and

sizes observed for NS (Online Resource Fig. S1). The mean hydrodynamic diameter of N25S, N25SS, and NS were 164 ± 86, 176 ± 96, and 414 ± 162 nm, respectively. This shows that shear-mixing reduced particle aggregates of N25SS slurry (compared to NS). Polydispersity of the nZVI samples was also confirmed by SEM imaging. A typical SEM micrograph is shown in Fig. S2 (Online Resource). nZVI particles are mostly spherical with some irregular-shaped particles. The BET surface area of dry NS particles was 17.542 ± 0.061 m^2/g, while the micropore area was determined to be 1.832 m^2/g. The XRD scans showed that the nZVI samples are mostly Fe^0 with some iron oxides (Online Resource Fig. S3). The peaks at $2\theta = 44.7°, 65.02°$, and 82.3 were assigned to Fe^0. Secondary peaks represent iron oxides. The magnetite and maghemite peaks are not easily distinguished by XRD because their cubic lattice parameters are very similar (Rojas et al. 2004). Peaks for FeO(OH), Fe_2O_3, and hydrated iron oxides were also observed. NS dry powder had very low amount of iron oxide.

Average particle diameter and count rate

We observed the largest particle sizes at the start of the experiments in both aerobic and anaerobic conditions (Table 1). This is mainly due to rapid aggregation caused by low electrostatic repulsion and magnetic attraction (Karn et al. 2009; O'Carroll et al. 2012). Magnetic attraction depends on the particle size to the sixth power (Phenrat et al. 2008). In the $CaCl_2$ and RW suspensions, aggregation was further promoted by screening of electrostatic repulsion by the cations (Li et al. 2006), thereby increasing the size and density of the nZVI and iron oxide particles in the supernatant of all the samples. Steric repulsion does not seem to improve the stability of N25S compared to NS and N25SS at the particle and electrolyte concentrations considered in this study. Other studies have observed significant aggregation in polymer-modified nZVI (Phenrat et al. 2010). However, previous work with bare nZVI indicated that the surfactant in N25S plays a major role in stabilizing the original particles at other conditions (Keller et al. 2012). Most of the particles measured were in the micrometer range on Day 0. The largest hydrodynamic particle sizes were observed in the RW suspensions on Day 0 while NanoPure water suspensions were generally the lowest in size. Due to size and density, the movement of micrometer-scale metal particles is largely controlled by gravity-induced sedimentation (Karn et al. 2009). nZVI and iron oxide particles have been shown to aggregate into clusters that are large enough to be affected by gravity within a couple of minutes (Phenrat et al. 2007; O'Carroll et al. 2012; Zhu et al. 2012). Gelation has also been reported in nZVI by other studies, in which nZVI form large networks of fractal aggregates, which further enhances gravitational sedimentation (Chang and Kang 2009; Phenrat et al. 2007).

As the larger aggregates settled out, progressively smaller particle sizes were observed in the supernatant over time. Reduction in particle size over time is also due to the oxidation of nZVI particles in the supernatant to soluble iron oxides. Aggregation rate may increase or decrease with time depending on the species of iron oxide formed and their magnetic properties (Phenrat et al. 2007). The hydrodynamic size of N25S and N25SS in NanoPure water was stable throughout the period of the experiment after the suspensions equilibrated but we observed no stability at higher ionic strength. The presence, species and concentration of groundwater cations in the remediation sites is expected to affect the stability and aggregation of the nZVI particles being applied (Saleh et al. 2008; Sun et al. 2007). Unlike N25SS, due to its large initial size and thus increased magnetic attraction, NS was not stable in any of the conditions, including NanoPure water. The hydrodynamic diameter of NS varied up to 3.6 μm throughout the study in all the conditions. This agrees with SEM, which showed that NS primarily exists as micron-sized aggregates (Online Resource Fig. S2), and would need to be dispersed before use for remediation. The instability of NS in any of the conditions studied underscores the role of initial particle size and pretreatment in nZVI stability and their overall behavior when they are introduced into the environment for pollution remediation (Karn et al. 2009; Mueller et al. 2012; Pan and Xing 2012).

Similar to size measurements, particle count rates were relatively constant in NanoPure water, but not in the $CaCl_2$ and RW suspensions. NS was not stable in any condition. The count rates for N25S and N25SS were one order of magnitude larger in NanoPure water compared to the other media, indicating higher suspension stability at low ionic strength. In general the count rate was lowest in the 100 mM $CaCl_2$ solution and

Table 1 Hydrodynamic diameter (nm) of aqueous suspensions of nZVI particles in aerobic and anaerobic conditions observed over a period of 28 days

Days	NanoPure water	10 mM $CaCl_2$	100 mM $CaCl_2$	RW	NanoPure water	10 mM $CaCl_2$	100 mM $CaCl_2$	RW
	N25S in aerobic condition (nm)				N25S in anaerobic condition (nm)			
0	2757.00	4336.67	3044.67	4153.00	944.10	3190.33	3398.67	7442.00
1	173.63	996.93	2317.67	1103.67	175.90	1932.67	1723.33	2550.33
2	187.33	1122.67	1212.50	1524.67	169.97	2529.67	2190.33	2713.00
4	161.60	1654.75	1.17	738.58	177.33	3123.00	ND	3537.00
7	176.10	ND	ND	859.73	165.53	381.80	0.33	134.78
14	285.03	ND	ND	ND	180.90	ND	ND	ND
28	170.60	173.50	ND	177.50	146.40	ND	ND	ND
	N25SS in aerobic condition (nm)				N25SS in anaerobic condition (nm)			
0	2512.33	396.10	2969.67	4302.67	608.93	2778.50	3185.00	3801.67
1	247.23	711.75	1493.67	6646.67	237.27	2302.67	3974.33	2745.00
2	222.80	771.90	1890.00	5016.00	212.77	2085.33	3514.67	3502.00
4	222.90	1689.00	799.37	0.68	206.80	2109.33	2919.33	2134.33
7	219.63	2437.00	ND	ND	239.23	3225.00	1451.40	2207.33
14	179.43	ND	ND	ND	181.17	1826.00	929.55	3326.33
28	155.30	ND	50.05	97.28	168.20	ND	ND	ND
	NS in aerobic condition (nm)				NS in anaerobic condition (nm)			
0	1864.33	1760.50	2469.67	3601.33	1003.33	2018.00	2813.00	3039.67
1	755.77	485.20	2160.33	974.90	658.23	861.00	1755.00	1549.00
2	965.27	0.00	2496.00	241.70	673.93	ND	1915.00	461.18
4	ND	1004.40	14.60	ND	1268.67	72.75	1618.83	ND
7	2056.00	8.16	ND	ND	6204.00	28.86	ND	1429.67
14	ND	ND	ND	ND	ND	ND	1052.25	ND
28	ND	1120.60	377.60	1066.83	ND	ND	ND	18.98

ND not detected

highest in NanoPure water (Fig. 1). Other suspended materials (different from nZVI) present in the groundwater sample may have contributed to the count rate we observed in RW, especially at the start of the experiment. In NanoPure water, the nZVI listed in increasing supernatant count rate are NS < N25S < N25SS. As shown in Online Resource Table S1, the count rate range observed in NS was 0.9–20.5 kilocounts per second (kcps) while N25SS and N25S were 1.0–234.6 and 1.0–133.0 kcps, respectively. The count rates in the anaerobic conditions were slightly higher than in the aerobic conditions. In most of the conditions, the highest count rate was observed within 48 h and count rate decreased steadily thereafter, except in NanoPure water. Aggregation (and thus sedimentation) occurs because van der Waals and magnetic attraction are stronger than the electrostatic and steric repulsions.

pH

nZVI is able to react with dissolved oxygen in water and to an extent with water as shown in Eqs. (1) and (2) below (Karn et al. 2009; Sun et al. 2006; Zhang 2003; Zhang and Elliott 2006):

$$2Fe^{0}_{(s)} + 4H^{+}_{(aq)} + O_{2(aq)} \rightarrow 2Fe^{2+}_{(aq)} + 2H_2O_{(l)} \quad (1)$$

$$Fe^{0}_{(s)} + 2H_2O_{(aq)} \rightarrow Fe^{2+}_{(aq)} + H_{2(g)} + 2OH^{-}_{(aq)} \quad (2)$$

$$4Fe^{2+}_{(aq)} + 4H^{+}_{(aq)} + O_{2(aq)} \rightarrow 4Fe^{3+}_{(aq)} + 2H_2O_{(l)} \quad (3)$$

In aerobic condition (1), nZVI is oxidized to ferrous iron and protons are consumed in the process. This

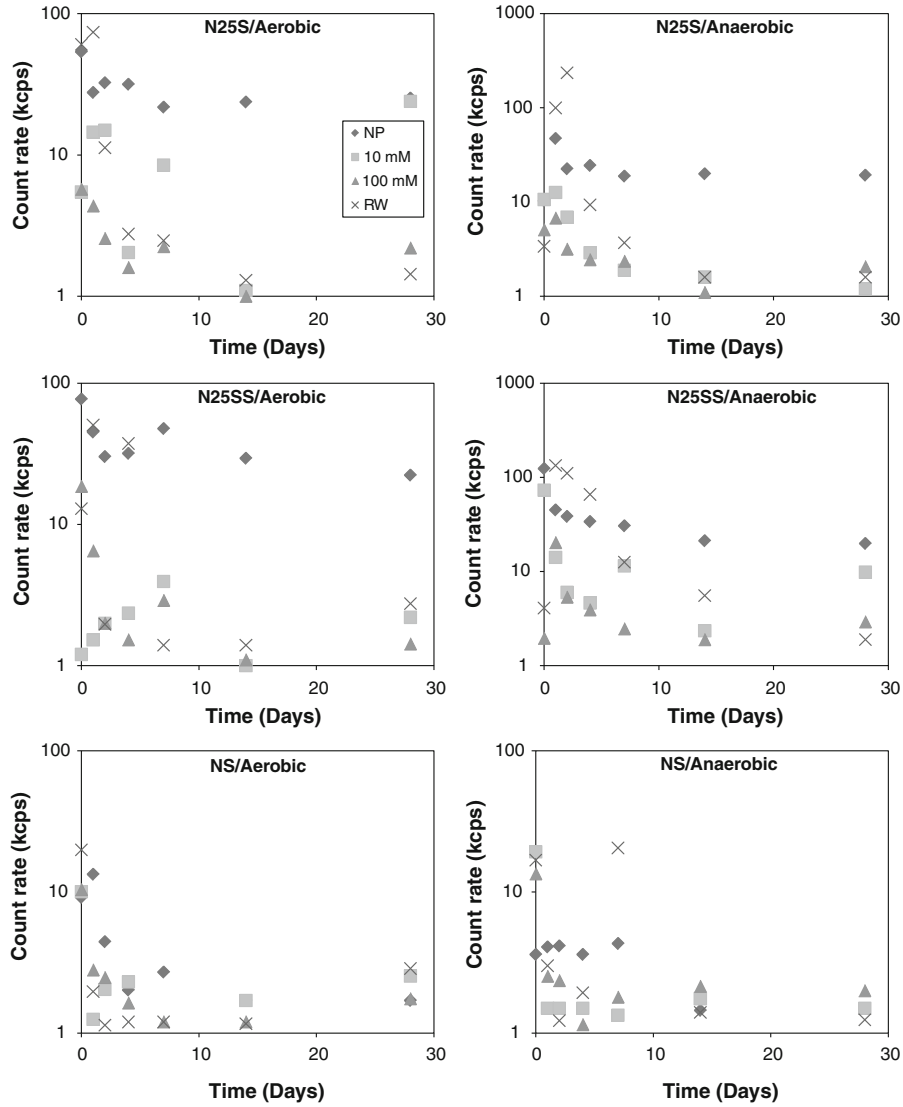

Fig. 1 The mean count rate (in kilo counts per second, kcps) obtained for nZVI particles (N25S, N25SS, and NS) aged for 28 days in aerobic and anaerobic conditions in NanoPure water (NP), 10 mM $CaCl_2$ (10 mM), 100 mM $CaCl_2$ (100 mM), and groundwater (RW)

reaction is thermodynamically favorable, with $E^0 = +1.71$ V at 25 °C (Zhang and Elliott 2006). In anaerobic or anoxic condition (2), nZVI reacts with water to produce ferrous iron, hydrogen gas, and alkalinity. Ferrous ions are further oxidized to ferric ions in the presence of oxygen (Eq. 3). These three reactions increase media pH. At the start of this study, we adjusted all the suspensions except RW to ~pH 7 to simulate the environmental pH range, but in NanoPure water the pH increased to 9.4–9.8 within minutes except for NS, which remained within the neutral range. NS has lower surface area for corrosion (compared to smaller N25SS and N25S) due to its larger primary particle size, and magnetic attraction. Previous studies also reported 2–3 U increase in pH within an hour after nZVI particles were introduced into distilled water, regardless of the nZVI concentration (Sun et al. 2006; Zhang 2003). A steady rise in pH was observed for all three nZVI particles in RW, which started out at ~pH 7 and reached pH >9. In fact, by Day 28 the highest pH readings (7.2–9.5) were observed in the RW conditions. In the RW controls,

the pH range was 7.1–8.2 for the aerobic condition and 6.4–7.9 for the anaerobic condition—both much lower than what was observed when nZVI was suspended in the groundwater. The slower rate of nZVI oxidation in RW (compared to NanoPure water) may be due to interaction of natural organic matter (NOM) in the groundwater with the surface of nZVI particles, reducing their reactivity (Dries et al. 2005; Giasuddin et al. 2007). However, the production of reactive oxygen species (ROS) during nZVI oxidation may lead to the oxidation of NOM (Matheson and Tratnyek 1994; Joo et al. 2004) and free up the reactive sites of the particles. As a result, we observed a progressive increase in pH in RW media over time. The presence of natural buffers in the environment may prevent a large pH increase in the environment, but a recent field study reported a slight increase in pH around the nZVI injection point (Wei et al. 2012).

The overall pH ranges observed in 10 and 100 mM $CaCl_2$ suspensions (6.3–9.0 and 6.0–8.7, respectively) were significantly lower than in NanoPure water (6.5–9.8) and RW (7.1–9.5). This may be due to reduced reactivity of nZVI particles as a result of surface passivation by Cl^-. It has been previously noted that Cl^- reduces surface reactivity of nZVI in water by forming Fe–Cl^- complexes on the iron surface, passivating the reactive sites (Sun et al. 2007; Liu et al. 2007). Groundwater anions such as Cl^- and PO_4^{2-} may serve as ligands because they have atoms with a lone pair of electrons that can be donated in a coordinate bond (Cornell and Schwertmann 2003; Liu et al. 2007; Sun et al. 2006). These ligands may adsorb to the outer iron oxide surface of nZVI either specifically (Eqs. 4, 5) or non-specifically (Eq. 6) (Cornell and Schwertmann 2003; Sun et al. 2006):

$$\equiv FeOH + L^- \leftrightarrow \equiv FeL + OH^- \quad (4)$$

$$\equiv (FeOH)_2 + L^- \leftrightarrow \equiv Fe_2L^+ + 2OH^- \quad (5)$$

$$\equiv FeOH + L^- + H^+ \leftrightarrow \equiv Fe(OH)_2 + L^- \quad (6)$$

where the symbols $\equiv$ and L^- represent the iron surface and anionic ligands, respectively.

Adsorption of ligands also leads to increase in pH (Eqs. 4–6). Increase in solution pH may further reduce the reactivity of nZVI particles through the formation of less soluble iron hydroxide-based precipitates on the surface (Matheson and Tratnyek 1994; Joo et al. 2004). The complete pH measurement data are presented in Online Resource Table S2.

Zeta potential

Zeta (ζ) potential of nanoparticles, i.e., their apparent surface charge, has been shown to strongly depend on solution pH. As nZVI corrodes, OH^- is produced (or H^+ is consumed) and ζ potential becomes more negative (Zhang and Elliott 2006). This is also marked by change in surface characterization as nZVI corrodes. The most negative ζ potential values were observed for the N25S and N25SS particles aged in NanoPure water and RW (Fig. 2). NS was also mostly (but less) negative in these two media. Following the pH trend observed in RW and Nanopure water, the ζ potential of the nZVI particles in the RW became more negative with time while the most negative values in NanoPure water were observed at the start of the experiment. The maximum ζ potential values observed for N25S suspended in water were -30 and -38 mV in aerobic and anaerobic conditions, respectively. For N25SS suspended in NanoPure water, maximum ζ potential values observed were -36 and -40 mV in aerobic and anaerobic conditions, respectively. There was more spread in the overall ζ potential range of NS in both NanoPure water and RW than for N25S and N25SS. For the $CaCl_2$ suspensions, the ζ potential values were much less negative compared to the observation in NanoPure water and RW. In fact, several positive values of ζ potential were observed for NS in $CaCl_2$ suspensions. The divalent cation, Ca^{2+}, screens the electrostatic charge on the surface of the iron nanoparticles (Li et al. 2006). In general, the trend observed for the nZVI ζ potential was: NanoPure water > RW > 10 mM $CaCl_2$ > 100 mM $CaCl_2$. The low ζ potentials in the $CaCl_2$ and RW suspensions (≥ -25 mV) implies that electrostatic repulsions between nZVI particles may be insignificant in groundwater, leading to aggregation and stronger attachment to natural mineral surfaces. These interactions may reduce the mobility and reactivity of the nZVI in the aquifer thereby increasing persistence.

Oxidation–reduction potential

The ORP of nZVI depends on (1) deposition of the particles on the redox electrode, and (2) the reactivity of nZVI in aqueous media (Shi et al. 2011). As such, the magnitude of ORP may be indicative of the aggregation state of nZVI in aqueous systems:

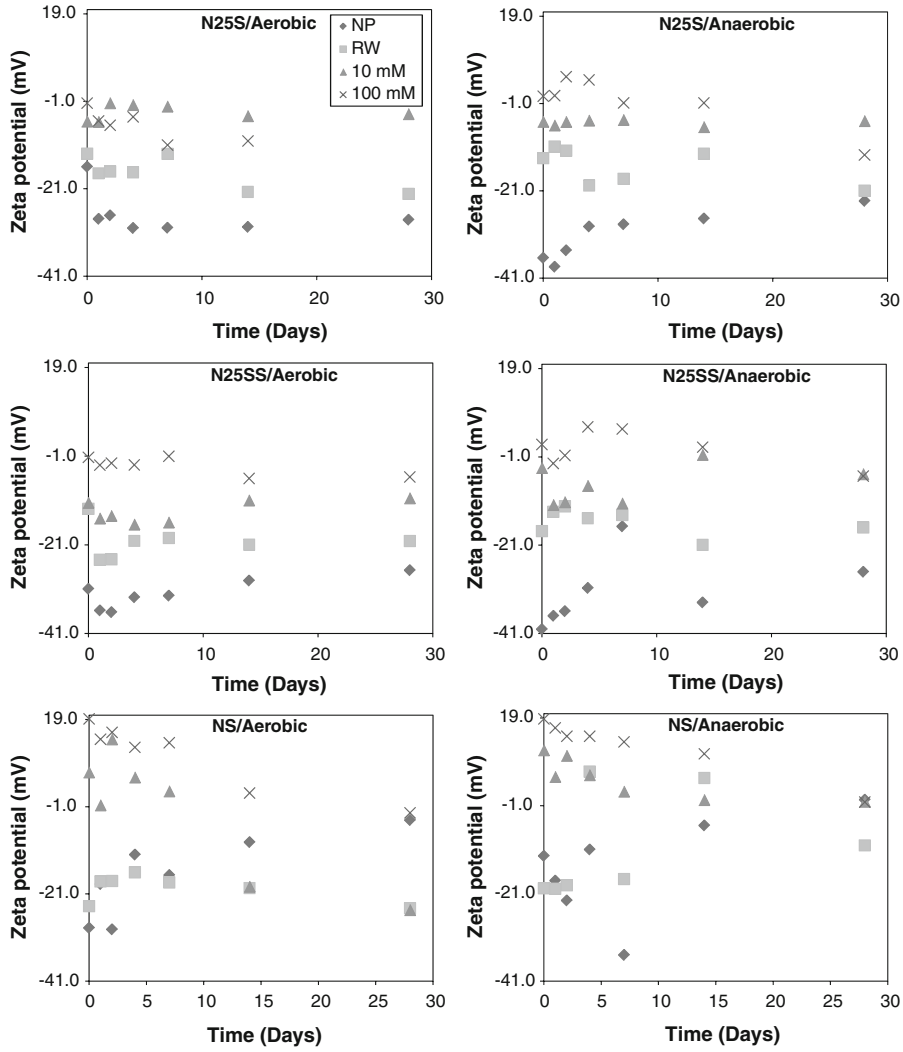

Fig. 2 Zeta (ζ) potential (mV) of nZVI particles aged for 28 days in NanoPure water (NP), 10 mM $CaCl_2$ (10 mM), 100 mM $CaCl_2$ (100 mM), and groundwater (RW) in aerobic and anaerobic conditions

Aggregated nZVI will sediment and not deposit significantly on the electrode. Also, aggregation reduces the surface area on nZVI, affecting the reactivity of nZVI. The ORP we observed in this study is indicative of aggregated nZVI particles, since the ORP measured is mainly due to Fe^{2+} from nZVI corrosion (Shi et al. 2011). N25S and N25SS showed consistently negative ORP in all four aqueous media throughout the period of the experiment (Fig. 3). In NanoPure water, ORP as low as −406 mV was observed in aerobic conditions, while in the anaerobic condition the lowest ORP measured in NanoPure water was −398 mV for the three nZVI particles. The ORPs observed in the $CaCl_2$ suspensions and RW were also very low despite the expected passivation by the electrolytes. This implies that high level of groundwater cations is unlikely to limit the ability of nZVI particles to create a reducing environment.

nZVI oxidation involves the consumption of oxygen (and other oxidants if present) and the production of Fe^{2+} and hydrogen, resulting in reducing conditions in the aqueous media (Sun et al. 2006; Zhang and Elliott 2006). This reducing condition persists as long as iron remains reactive and water is available (Sun et al. 2006). There was evidence of nZVI reactivity throughout the 28-day period of this study and in another study we observed reactivity for up to 60 days. The ORP of NS showed that the as-received dry nanoparticles were less reactive than the shear-mixed aqueous N25S and N25SS, releasing the ferrous ions more slowly. The ORP values observed suggest that the consumption of oxidants in NS suspensions is

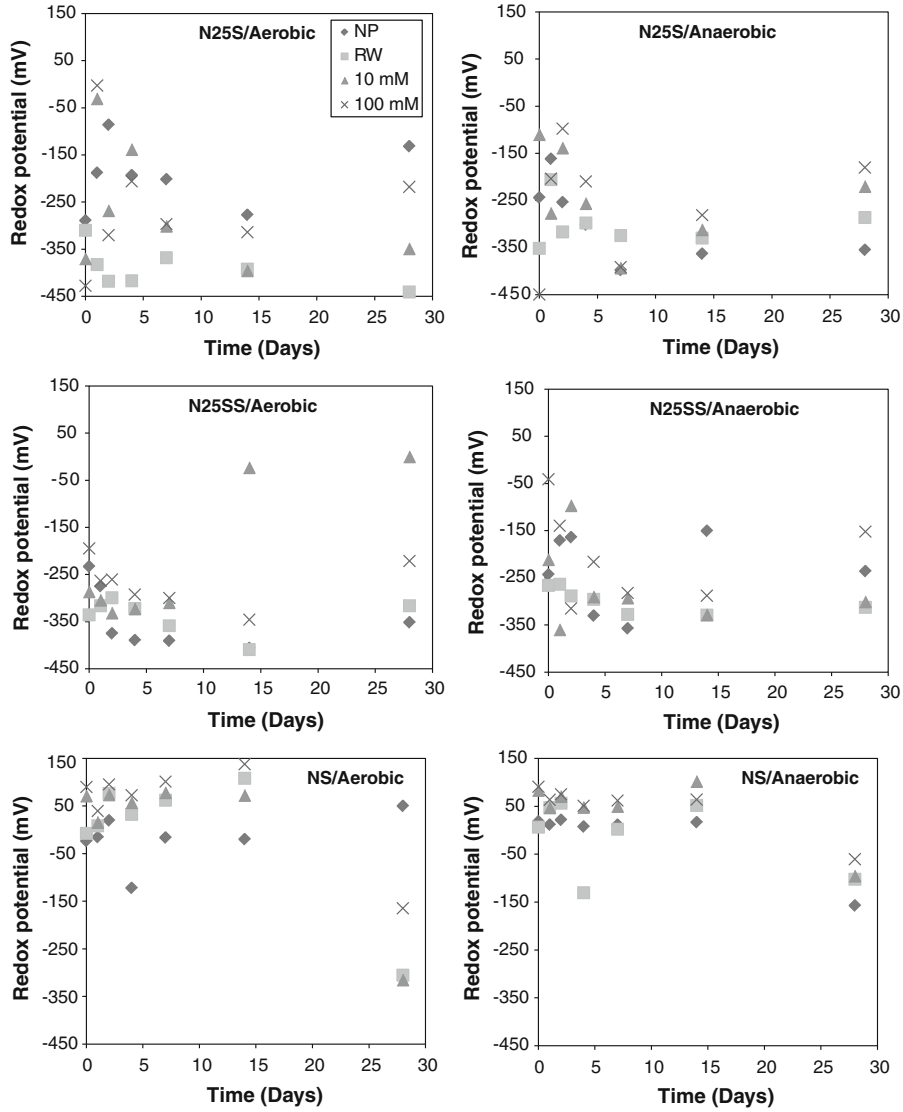

Fig. 3 Oxidation–reduction potential (ORP) of nZVI suspensions in NanoPure water (NP), 10 mM $CaCl_2$ (10 mM), 100 mM $CaCl_2$ (100 mM), and groundwater (RW) in aerobic and anaerobic condition

slower and lower than in suspensions of N25S and N25SS when all three nZVI are aged for a month.

Several bench and field studies have demonstrated that iron-based nanoparticles can establish low-negative ORP in water and soil within minutes (Chang and Kang 2009; Sun et al. 2006; Zhang 2003; Wei et al. 2010) and ORP reduction may be concentration-dependent (Chang and Kang 2009; Shi et al. 2011; Sun et al. 2006). In a field study, ORP of −700 mV was observed after the introduction nZVI into an injection well with initial ORP of +50 to −100 mV (Zhang and Elliott 2006). The reduction of the groundwater and soil ORP is very important for the transformation of many persistent pollutants such as chlorinated organic compounds and pyrene (Chang and Kang 2009; Zhang and Elliott 2006; Wei et al. 2010).

Fe concentration in different phases

In addition to the measured concentration of various iron species, we observed major color changes (mostly from black to green, and the rusty coloration of Fe^{3+}) in both the supernatant and the upper layer of the sediment phases of N25S and N25SS. NS remained

almost completely black up until Day 28 (Online Resource Fig. S4). Some faint rusty coloration was observed in the sediment of NS at Day 28. After Day 28, this rusty coloration increased over time. Ferrous iron in the supernatant and total iron in the supernatant, suspended sediment and the sediment phases were monitored.

Total dissolved (supernatant) Fe concentration

$[Fe]_{total}$ in the supernatant is expected to change as a result of (1) oxidation of nZVI to soluble iron species; (2) transformation of soluble iron to insoluble iron species like FeOOH, and Fe_3O_4; and (3) aggregation-induced sedimentation of nZVI and iron oxides (Karn et al. 2009; Phenrat et al. 2007). In the $CaCl_2$ suspensions, these processes are affected by the presence of dissolved ions, which may result in passivation, complexation, and increased aggregation. nZVI oxidation results in the formation of ferrous iron (1 and 2), which can then be further oxidized to ferric iron (Eq. 3), magnetite (Eq. 7), or ferrous hydroxide (Eq. 8), depending on redox conditions and pH. Furthermore, ferric iron can undergo hydroxylation to form ferric hydroxide (Eq. 9). It may also react with water to form oxyhydroxide (Eq. 10). Ferric hydroxide may lose water to form oxyhydroxide (Eq. 11). Transformations may also occur between iron hydroxides and magnetite (Eqs. 12, 13) (Li et al. 2006; Kanel et al. 2005).

$$6Fe^{2+} + O_2 + 6H_2O \rightarrow 2Fe_3O_4 + 12H^+ \quad (7)$$

$$Fe^{2+} + 2OH^- \rightarrow Fe(OH)_2 \quad (8)$$

$$Fe^{3+} + 3OH^- \rightarrow Fe(OH)_3 \quad (9)$$

$$Fe^{3+} + 2H_2O \rightarrow FeOOH + 3H^+ \quad (10)$$

$$Fe(OH)_3 + 3H^+ \rightarrow FeOOH + H_2O \quad (11)$$

$$6Fe(OH)_2 + O_2 \rightarrow 2Fe_3O_4 + 6H_2O \quad (12)$$

$$4Fe_3O_4 + O_2 + 18H_2O \leftrightarrow 12Fe(OH)_3 \quad (13)$$

These iron species may be present in the supernatant as ions or particulates which may eventually sediment out. Several studies have reported the presence of iron oxides such as FeO (Sun et al. 2006), γ-Fe_2O_3 (Li et al. 2006) and Fe_3O_4 (Li et al. 2006; Phenrat et al. 2007) on the surface of nZVI, with the oxide layer growing as the nZVI ages (Sun et al. 2006). We confirmed the presence of FeO(OH), Fe_2O_3, γ-Fe_2O_3, and Fe_3O_4 on the surface of nZVI used for this study (Online Resource Fig. S3). The type of oxide present on the shell of nZVI depends on how it is produced and the prevalent environmental condition (Li et al. 2006).

The concentrations of soluble iron species decreased exponentially in most of the conditions over time (Fig. 4). The soluble iron concentration observed over time depends on (1) the rate of oxidation of nZVI to soluble iron species; and (2) the rate of transformation of the soluble iron to insoluble species. Both rates are affected by the surface characteristics of the nZVI particle, nature of media, pH, availability of oxidants, etc. For instance, both the oxidation of the nZVI phase and the transformation of the soluble iron phase are expected to be slowed by Cl^- in the $CaCl_2$ suspensions. This may result in either increase or decrease in soluble iron concentration depending on reaction rate of both phases and how much the presence of Cl^- impacts the rates. In general, however, the oxidation rate of nZVI is expected to decrease with time as the reaction sites are used up while the formation of insoluble iron species are favored by the increase in pH and the availability of reactants. As a result the decrease in dissolved iron concentration of the supernatant can be attributed to the formation of insoluble iron oxides (oxides, hydroxides, and oxyhydroxides), which either remain suspended or settle out into the sediment phase of the suspensions. The rate of supernatant iron reduction appears to be directly proportional to the initial concentration of soluble iron species detected in the different suspensions. The nZVI suspensions that had low soluble iron concentration on Day 0 ($\leq$1.0 mg/L) did not vary as much over time while those with high initial iron concentration (>1.0 mg/L) decreased exponentially (Fig. 4).

Dissolution increases bioavailability of metals (Hogstrand and Wood 1998), presenting a potential toxicity route. For instance, dissolved Fe^{2+} (especially at high levels) has demonstrated bactericidal activities by (1) inducing oxidative stress (Auffan et al. 2008), and (2) precipitation of ferric hydroxide nanoparticles in the cytoplasm, leading to cell destruction (Marsalek et al. 2012). Toxicity due to dissolved iron species will be most significant right after nZVI injection, when high levels of the species were determined (Fig. 4).

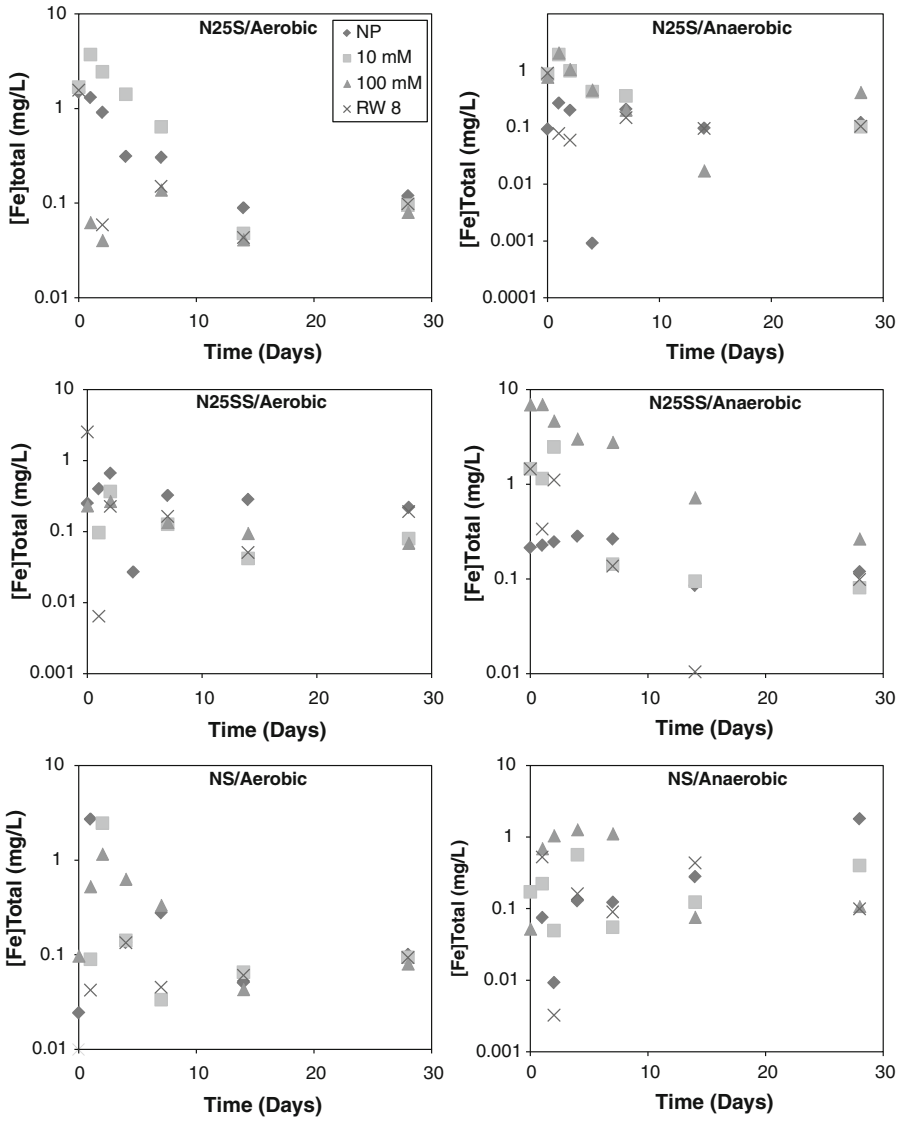

Fig. 4 Total dissolved iron concentration ($[Fe]_{total}$) in the supernatant of nZVI suspensions aged in NanoPure water (NP), 10 mM $CaCl_2$ (10 mM), 100 mM $CaCl_2$ (100 mM), and groundwater (RW) in aerobic and anaerobic conditions

Suspended Fe concentration

The suspended sediment iron category includes all the insoluble iron species that form small particulates. This includes unoxidized and partially oxidized nZVI, and the insoluble iron oxides, hydroxides, and oxyhydroxides such as FeO, Fe_2O_3, FeOOH, and Fe_3O_4; formed as described by Eqs. (7–13). Similar to the observation in the supernatant total iron, the concentration of the suspended particles decreased exponentially over time except in NanoPure water, in which particle concentration appeared to be steady for the period of this study (Fig. 5). The same trend was observed in the particle size data that was obtained via DLS—hydrodynamic diameter of particles increased for the first few days and then decreased sharply in all the media except in NanoPure water. NS was not stable in any of the aqueous suspensions, including NanoPure water. Online Resource Table S3 shows the Day 1 and Day 28 iron levels measured in the suspended sediment of all the nZVI conditions. The average concentration of iron detected in the

suspended sediment of NanoPure water suspension of N25S after Day 0 was ~4.5 g/kg, while we observed ~2.5 and ~0.05 g/kg for N25SS and NS, respectively, in the same condition. As expected, we observed more sedimentation in the ionic media. For instance, in the aerobic 10 mM $CaCl_2$ condition, iron concentration in the suspended sediment of N25S decreased from 0.2 g/kg on Day 1 to 0.004 g/kg on Day 28. Under the same condition, N25SS decreased from 0.01 g/kg on Day 1 to undetectable levels on Day 28. While stability was observed in the NanoPure water after the suspension equilibrated on Day 0, the presence of Ca^{2+} screened the electrostatic repulsion among the iron particulates, causing them to aggregate more and sediment. RW had an ionic strength of ~46 mM (Online Resource Table S4). As such, rapid aggregation was also expected in RW. Sedimentation of iron particulates is expected to occur in the subsurface following nZVI injection. Sedimentation may however be limited by interception/adsorption to soil moieties and straining of the large aggregates. Wei and coworkers reported accumulation of iron in the upper layer of an injection site, which reduced significantly after a storm event (Wei et al. 2010). Straining is significant when the ratio of the particle (nZVI) diameter to porous media grain diameters exceeds 0.05 (Sakthivadivel 1969; Auset and Keller 2006). Significant straining has been demonstrated when the ratio is as low as 0.003 (Bradford et al. 2007). The presence of iron particulates may therefore affect the soil/aquifer characteristics such as permeability and transport (Phenrat et al. 2007; Ponder et al. 2000; Saleh et al. 2007; Schrick et al. 2004; Reddi et al. 2000; Liu et al. 2007; Wei et al. 2010).

Sediment Fe concentration

The sediment phase was the reservoir for nZVI and iron oxide particulates that settled out of the suspension. In aerobic conditions, the range of iron detected in the sediment was 13–540 g/kg while in anaerobic the range was 33–523 g/kg. The lowest iron concentrations were determined in the sediment on the first day of the study (Day 0) when the initial settling was still going on and it remained relatively stable thereafter (Fig. 6). Although the suspended iron decreased rapidly, the reason we did not observe a concurrent rapid increase in the sediment iron after Day 1 is because the concentration of iron in sediment was several orders of magnitudes higher than concentrations of suspended particles. In addition, the increase in sediment iron may not be easy to monitor because the sediment phase is not evenly spread out and it is difficult to obtain a representative sample from the deposits. Also, continuous sampling from the sediment phase reduced the amount of iron in the sediment and caused minor disturbance that may have further increased the unevenness of the sediment phase.

We observed that oxidation of nZVI and by-products also took place in the sediment phase. This was evidenced by (1) the change in the coloration of the sediment phase, progressively from the top layer; and (2) the observed trend in the ferrous iron concentration monitored in the supernatant (discussed below). Sedimentation of particulate nZVI and its by-products to the sediment phase of the aquifer may increase the local concentration of redox-active iron species around the injection well, which may significantly affect the aquifer's geochemistry, and sediment biota. Some of the possible effects are discussed in the implication section.

Supernatant ferrous concentration

Fe^{2+} is expected to be one of the first products in the oxidation series of nZVI. However, Fe^{2+} is only a transition state since it can be further oxidized to other forms, mainly Fe^{3+}. As such, the amount of Fe^{2+} detected in the nZVI suspension is proportional to the rate of nZVI oxidation and indirectly proportional to the rate of Fe^{2+} oxidation. For Fe^{2+} concentration measurements, we did not separate the suspended iron particulates from the supernatant. This is expected to influence the result since insoluble Fe^{2+} species (e.g., FeO) may be present in the suspension. However, insoluble Fe^{2+} is likely much less reactive than dissolved Fe^{2+}. Also, any nZVI particles present in the suspended sediment may be oxidized in water to produce more Fe^{2+} during analysis. The highest Fe^{2+} concentration in all the conditions was measured at the start of the experiment (Fig. 7). In the $CaCl_2$ and RW suspensions of N25S and N25SS, the concentration of Fe^{2+} increased steadily after Day 1, peaked around Day 2–3 and then decreased. A similar pattern was observed in NanoPure water, but there was less variability from Day 1 to 28. The decrease in the Fe^{2+} concentration by Day 1 indicates that Fe^{2+} oxidation exceeded the rate of nZVI oxidation after Day 0.

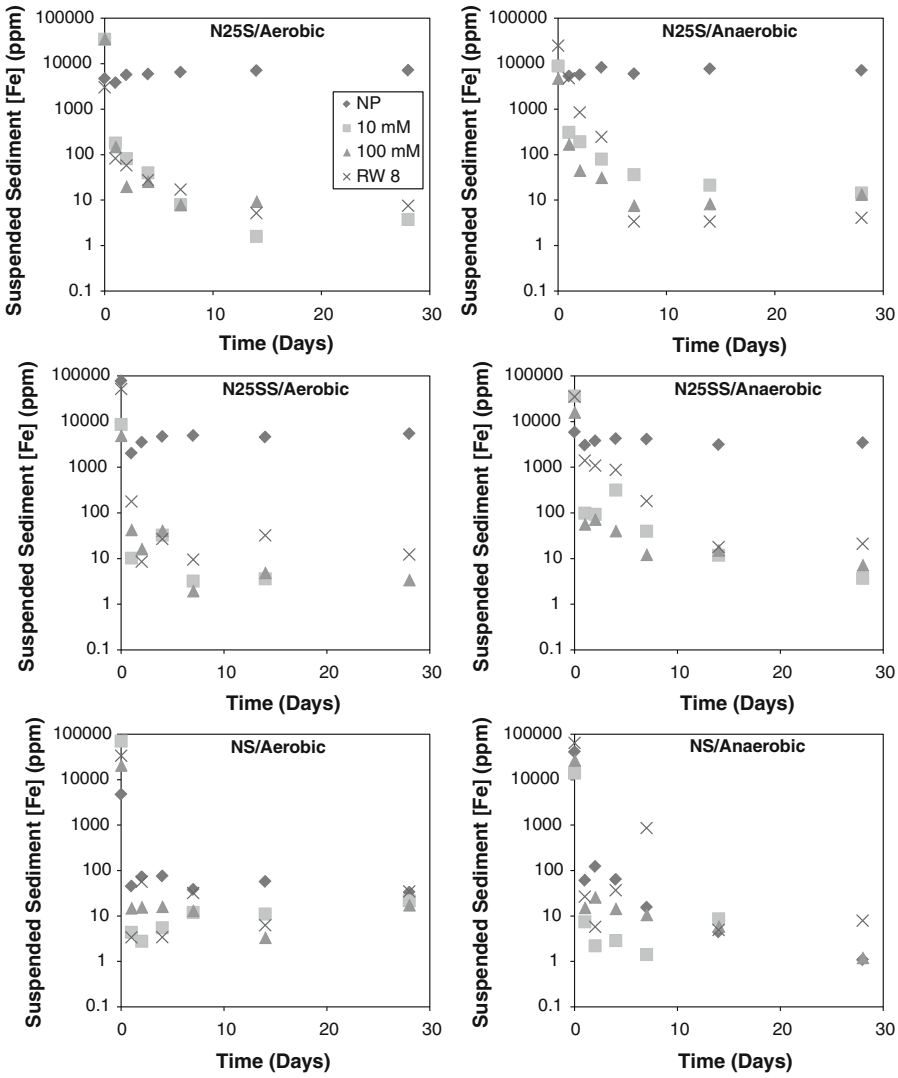

Fig. 5 Total iron concentration of particles suspended in the supernatant after 28 days, in NanoPure water (NP), 10 mM $CaCl_2$ (10 mM), 100 mM $CaCl_2$ (100 mM), and groundwater (RW) in aerobic and anaerobic conditions. The particulate iron concentration accounts for nZVI (unoxidized and partially oxidized), iron oxides, iron hydroxides, and iron oxyhydroxides suspended in the supernatant

The highest Fe^{2+} concentration was detected in the 100 mM $CaCl_2$ media for all conditions. The 10 mM $CaCl_2$ media had the next highest concentration in most of the conditions while the overall least concentration was observed in RW. The high Fe^{2+} in the $CaCl_2$ suspensions can be attributed to the interactions between the Fe^{2+} and the Cl^-. Anions can interact with Fe^{2+} in different ways, including the formation of ion pairs (Eq. 14), and complexation or catalysis (Millero 1985):

$$Fe^{2+} + C1^- \rightarrow FeC1^+ \quad (14)$$

$FeCl^+$ and $FeC1_2$ ion pairs are not easily oxidized. As a result, their formation reduces the oxidation rate of Fe^{2+} (Millero 1985, 1989). Also, the oxidation of Fe^{2+} is strongly correlated with solution pH (Millero 1985). As shown earlier, pH was lower in the $CaCl_2$ suspensions. As such, a slower rate of Fe^{2+} oxidation is expected in these conditions. The pH of the groundwater sample, RW, increased with time. This correlates with increasing Fe^{2+} oxidation rate, which agrees with our observation. Groundwater anions and pH thus play important roles in the speciation of iron.

The Fe^{2+} concentration measurement provides evidence for the oxidation of nZVI particles in and/or from the sediment phase and the lower reactivity of the particulate NS. We observed a slight increase in Fe^{2+} concentration around Day 2-3 in most of the

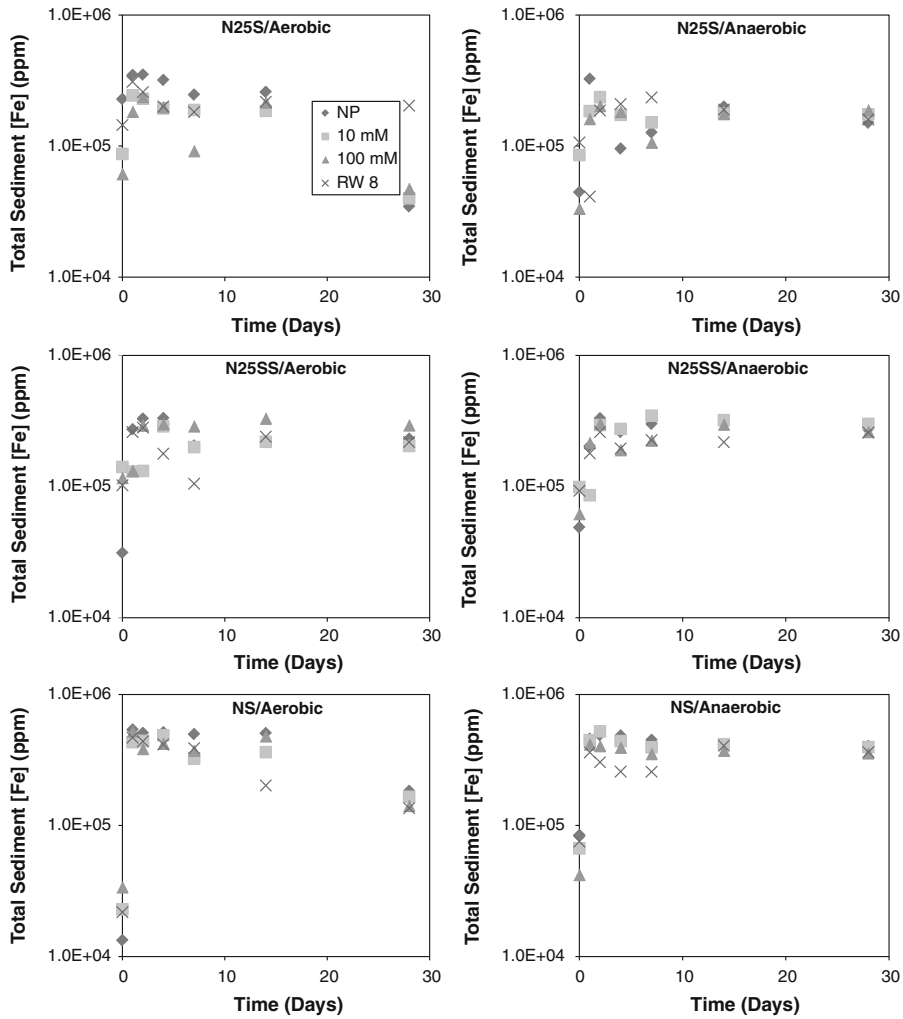

Fig. 6 Total iron concentration of the sediment phase after 28 days in NanoPure water (NP), 10 mM $CaCl_2$ (10 mM), 100 mM $CaCl_2$ (100 mM), and groundwater (RW) in aerobic and anaerobic conditions. The particulate iron in the sediment includes nZVI (unoxidized and partially oxidized), iron oxides, iron hydroxides, and iron oxyhydroxides

conditions. This slight increase is due to oxidation of nZVI particles in the sediment phase or the re-suspension of nZVI particles from the sediment phase, which then was oxidized in the supernatant.

For NS we observed significant Fe^{2+} concentration at the start of the study, like in the other nZVI particles. But unlike the other nZVI media, the Fe^{2+} concentration in NS suspensions dropped abruptly by Day 1 and remained low throughout this study. The concentration range observed in NS from Day 2 to 28 was 0–2 mg/L. Compared to the range observed in N25S (0–56 mg/L) and N25SS (0–83 mg/L), NS was much less reactive. Additional sampling done (data not shown) showed that the Fe^{2+} concentration remained insignificant in the NS media beyond 2 months.

Conclusions and implications for nZVI-mediated remediation

Similar to what occurs when the primary particle size is large, increased aggregation of nZVI and by-products by groundwater cations decreases the surface area available for reactivity. Reduced reactivity implies increased persistence of the iron particulates. Groundwater anions like Cl^-, HCO^{3-}, and PO_4^{2-} may also increase persistence of nZVI by forming coordinate bond with the outer iron oxide layer, thereby passivating the particles. Anion complexation and reduced reactivity may result in less negative zeta potential, more aggregation of the iron particulates, increased adsorption to the soil clay particles, and

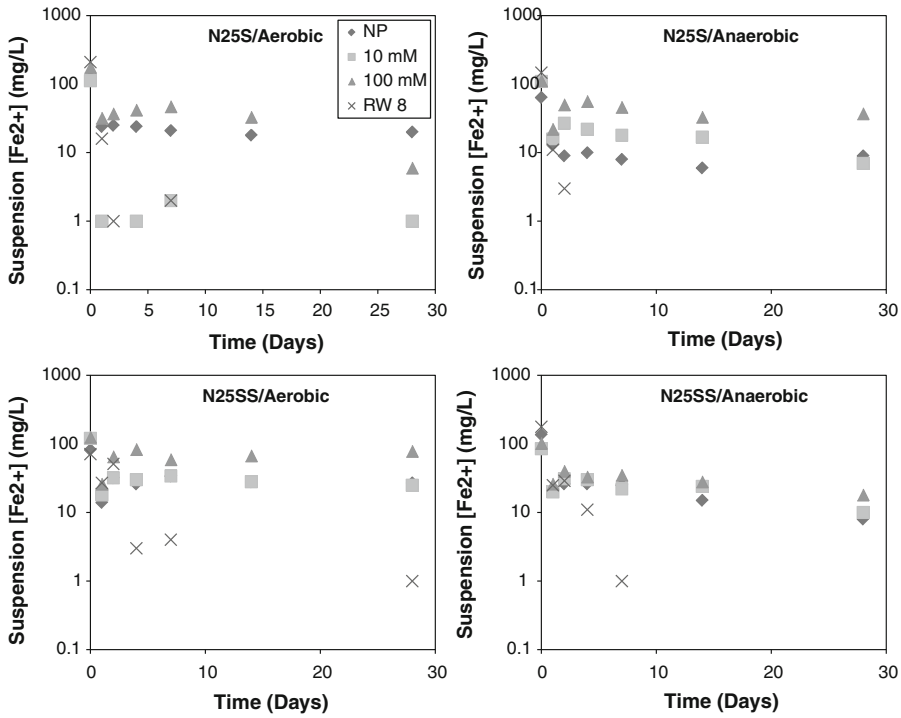

Fig. 7 Ferrous iron concentration in N25S and N25SS suspensions aged in NanoPure water (NP), 10 mM $CaCl_2$ (10 mM), 100 mM $CaCl_2$ (100 mM), and groundwater (RW) in aerobic and anaerobic conditions. Ferrous iron concentrations observed in NS are not shown because the values were insignificant after the initial (Day 0) surge

thus, less availability. All of these processes may contribute to increased persistence of nZVI and iron oxides in the soil matrix.

The sudden surge in the concentration of iron in the sediment beyond the natural levels may have adverse effects on living organisms there, many of which have important ecosystem functions. Although nZVI is not expected to be universally bactericidal (Kirschling et al. 2010; Chen et al. 2011a), ROS are produced during nZVI oxidation (Matheson and Tratnyek 1994; Joo et al. 2004) and by iron oxide nanoparticles (Buyukhatipoglu and Clyne 2011; Bennett and Keller 2011). nZVI particles and ferrous iron have been shown to cause oxidative stress in bacteria (Auffan et al. 2008), and affect growth of algae, invertebrates, and fish (Keller et al. 2012; Chen et al. 2011b; El-Temsah and Joner 2012; Marsalek et al. 2012). These two iron forms are the dominant species present immediately after the injection of nZVI into the ground, and under anaerobic conditions may persist for a significant amount of time, potentially breaking through to nearby surface water bodies. As shown in this study, ferrous iron may also persist depending on the ionic strength and the pH of the aquifer. Toxicity has also been demonstrated by iron oxide nanoparticles (Buyukhatipoglu and Clyne 2011; Zhu et al. 2012; Wang et al. 2011). In addition, the ability of nZVI to change the solution chemistry may significantly impact the microbial community around the injection wells and the radii of influence. This impact may go beyond to the point of injection as nZVI particles have been shown to flow with groundwater up to a distance of 20 m (Li et al. 2006; Sun et al. 2007; Zhang 2003). Downstream dilution of nZVI and by-products is however expected to reduce their effects on water chemistry away from the injection well (Wei et al. 2012). The extent of the change in solution chemistry has also been shown in this study to depend on the inherent characteristics of the aquifer in terms of the ions present, ionic strength, NOM, and pH.

In summary, this study showed that:

- Larger nZVI aggregates tend to be more persistent due to decreased reactivity;
- Groundwater ions and natural organic materials may increase the persistence of nZVI in the subsurface via reduced reactivity and surface passivation;
- The bulk of nZVI injected into the aquifer will eventually transform into iron oxide particulates, which will sediment out or get trapped in soil pores; and

- Groundwater chemistry is impacted by nZVI injection.

This implies that injection of nZVI into the ground should be preceded by proper evaluation of the specific site to be able to project the possible changes the nZVI injection may cause as well how this may influence the ecosystem.

Acknowledgments This study was supported in part by the National Science Foundation and the U.S. Environmental Protection Agency under Cooperative Agreement # NSF-EF0830117, and by the National Science Foundation Grant EF-0742521. It was also supported in part by a grant from AECOM. Any opinions, findings, and conclusions or recommendations expressed in this material are those of the authors and do not necessarily reflect the views of the National Science Foundation, the U.S. Environmental Protection Agency or AECOM. We thank the MRL Central Facilities for the use of their ICP-AES instrument. The MRL Central Facilities are supported by the MRSEC Program of the NSF under Award No. DMR05-20415, and DMR-1121053. We also thank Brittany Hall for her help in sampling and doing some of the ICP-AES measurements.

References

Amir A, Lee W (2011) Enhanced reductive dechlorination of tetrachloroethene by nano-sized zero valent iron with vitamin B12. Chem Eng J 170(2–3):492–497. doi:10.1016/j.cej.2011.01.048

Auffan M, Achouak W, Rose J Jr, Roncato M-A, Chanéac C, Waite DT, Masion A, Woicik JC, Wiesner MR, Bottero J-Y (2008) Relation between the redox state of iron-based nanoparticles and their cytotoxicity toward *Escherichia coli*. Environ Sci Technol 42(17):6730–6735. doi:10.1021/es800086f

Auset M, Keller AA (2006) Pore-scale visualization of colloid straining and filtration in saturated porous media using micromodels. Water Resour Res 42(12):W12S02. doi:10.1029/2005wr004639

Bennett SW, Keller AA (2011) Comparative photoactivity of CeO_2, γ-Fe_2O_3, TiO_2 and ZnO in various aqueous systems. Appl Catal B Environ 102(3–4):600–607. doi:http://dx.doi.org/10.1016/j.apcatb.2010.12.045

Bradford SA, Torkzaban S, Walker SL (2007) Coupling of physical and chemical mechanisms of colloid straining in saturated porous media. Water Res 41(13):3012–3024. doi:10.1016/j.watres.2007.03.030

Buyukhatipoglu K, Clyne AM (2011) Superparamagnetic iron oxide nanoparticles change endothelial cell morphology and mechanics via reactive oxygen species formation. J Biomed Mater Res A 96A(1):186–195. doi:10.1002/jbm.a.32972

Chang MC, Kang HY (2009) Remediation of pyrene-contaminated soil by synthesized nanoscale zero-valent iron particles. J Environ Sci Health A 44(6):576–582. doi:10.1080/10934520902784609

Chen JW, Xiu ZM, Lowry GV, Alvarez PJJ (2011a) Effect of natural organic matter on toxicity and reactivity of nano-scale zero-valent iron. Water Res 45(5):1995–2001. doi:10.1016/j.watres.2010.11.036

Chen P-J, Su C-H, Tseng C-Y, Tan S-W, Cheng C-H (2011b) Toxicity assessments of nanoscale zerovalent iron and its oxidation products in medaka (*Oryzias latipes*) fish. Mar Pollut Bull 63(5–12):339–346. doi:10.1016/j.marpolbul.2011.02.045

Cornell RM, Schwertmann U (2003) The iron oxides: structure, properties, reactions, occurrences, and uses. Wiley-VCH, Weinheim

Crane RA, Scott TB (2012) Nanoscale zero-valent iron: future prospects for an emerging water treatment technology. J Hazard Mater 211–212:112–125. doi:10.1016/j.jhazmat.2011.11.073

Dries J, Bastiaens L, Springael D, Kuypers S, Agathos SN, Diels L (2005) Effect of humic acids on heavy metal removal by zero-valent iron in batch and continuous flow column systems. Water Res 39(15):3531–3540. doi:10.1016/j.watres.2005.06.020

El-Temsah YS, Joner EJ (2012) Ecotoxicological effects on earthworms of fresh and aged nano-sized zero-valent iron (nZVI) in soil. Chemosphere 89(1):76–82. doi:10.1016/j.chemosphere.2012.04.020

Fan J, Guo YH, Wang JJ, Fan MH (2009) Rapid decolorization of azo dye methyl orange in aqueous solution by nanoscale zerovalent iron particles. J Hazard Mater 166(2–3):904–910. doi:10.1016/j.jhazmat.2008.11.091

Francis AJ, Dodge CJ (1998) Remediation of soils and wastes contaminated with uranium and toxic metals. Environ Sci Technol 32(24):3993–3998. doi:10.1021/es9803310

Giasuddin A, Kanel S, Choi H (2007) Adsorption of humic acid onto nanoscale zerovalent iron and its effect on arsenic removal. Environ Sci Technol 41(6):2022–2027. doi:10.1021/es0616534

Grieger KD, Fjordboge A, Hartmann NB, Eriksson E, Bjerg PL, Baun A (2010) Environmental benefits and risks of zero-valent iron nanoparticles (nZVI) for in situ remediation: risk mitigation or trade-off? J Contam Hydrol 118(3–4):165–183. doi:10.1016/j.jconhyd.2010.07.011

He F, Zhao DY (2005) Preparation and characterization of a new class of starch-stabilized bimetallic nanoparticles for degradation of chlorinated hydrocarbons in water. Environ Sci Technol 39(9):3314–3320. doi:10.1021/Es048743y

Hogstrand C, Wood C (1998) Toward a better understanding of the bioavailability, physiology and toxicity of silver in fish: implications for water quality criteria. Environ Toxicol Chem 17(4):547–561. doi:10.1897/1551-5028(1998)017<0547:TABUOT>2.3.CO;2

Holland KS (2011) A framework for sustainable remediation. Environ Sci Technol 45(17):7116–7117. doi:10.1021/es202595w

Jiemvarangkul P, Zhang W-X, Lien H-L (2011) Enhanced transport of polyelectrolyte stabilized nanoscale zero-valent iron (nZVI) in porous media. Chem Eng J 170(2–3):482–491. doi:10.1016/j.cej.2011.02.065

Joo SH, Zhao D (2008) Destruction of lindane and atrazine using stabilized iron nanoparticles under aerobic and anaerobic

conditions: effects of catalyst and stabilizer. Chemosphere 70(3):418–425. doi:10.1016/j.chemosphere.2007.06.070

Joo SH, Feitz AJ, Sedlak DL, Waite TD (2004) Quantification of the Oxidizing capacity of nanoparticulate zero-valent iron. Environ Sci Technol 39(5):1263–1268. doi:10.1021/es048983d

Kanel SR, Manning B, Charlet L, Choi H (2005) Removal of arsenic(III) from groundwater by nanoscale zero-valent iron. Environ Sci Technol 39(5):1291–1298. doi:10.1021/Es048991u

Kanel SR, Grenèche J-M, Choi H (2006) Arsenic(V) Removal from groundwater using nano scale zero-valent iron as a colloidal reactive barrier material. Environ Sci Technol 40(6):2045–2050. doi:10.1021/es0520924

Karn B, Kuiken T, Otto M (2009) Nanotechnology and in situ remediation: a review of the benefits and potential risks. Environ Health Perspect 117(12):1823–1831. doi:10.1289/Ehp.0900793

Keller A, Garner K, Miller R, Lenihan H (2012) Toxicity of nano-zero valent iron to freshwater and marine organisms. Plos One 7(8). doi:10.1371/journal.pone.0043983

Kirchner JW, Austin CM, Myers A, Whyte DC (2011) Quantifying remediation effectiveness under variable external forcing using contaminant rating curves. Environ Sci Technol 45(18):7874–7881. doi:10.1021/es2014874

Kirschling TL, Gregory KB, Minkley EG, Lowry GV, Tilton RD (2010) Impact of nanoscale zero valent iron on geochemistry and microbial populations in trichloroethylene contaminated aquifer materials. Environ Sci Technol 44(9):3474–3480. doi:10.1021/Es903744f

Li XQ, Elliott DW, Zhang WX (2006) Zero-valent iron nanoparticles for abatement of environmental pollutants: materials and engineering aspects. Crit Rev Solid State 31(4):111–122. doi:10.1080/10408430601057611

Liu Y, Phenrat T, Lowry GV (2007) Effect of TCE concentration and dissolved groundwater solutes on NZVI-promoted TCE dechlorination and H_2 evolution. Environ Sci Technol 41(22):7881–7887. doi:10.1021/es0711967

Marsalek B, Jancula D, Marsalkova E, Mashlan M, Safarova K, Tucek J, Zboril R (2012) Multimodal Action and selective toxicity of zerovalent iron nanoparticles against cyanobacteria. Environ Sci Technol 46(4):2316–2323. doi:10.1021/es2031483

Matheson LJ, Tratnyek PG (1994) Reductive dehalogenation of chlorinated methanes by iron metal. Environ Sci Technol 28(12):2045–2053

Millero FJ (1985) The effect of ionic interactions on the oxidation of metals in natural-waters. Geochim Cosmochim Acta 49(2):547–553

Millero FJ (1989) Effect of ionic interactions on the oxidation of Fe(Ii) and Cu(I) in natural-waters. Mar Chem 28(1–3): 1–18. doi:10.1016/0304-4203(89)90183-7

Mueller N, Braun J, Bruns J, Cernik M, Rissing P, Rickerby D, Nowack B (2012) Application of nanoscale zero valent iron (NZVI) for groundwater remediation in Europe. Environ Sci Pollut Res 19(2):550–558. doi:10.1007/s11356-011-0576-3

O'Carroll D, Sleep B, Krol M, Boparai H, Kocur C (2012) Nanoscale zero valent iron and bimetallic particles for contaminated site remediation. Adv Water Resour. doi:10.1016/j.advwatres.2012.02.005

Otto M, Floyd M, Bajpai S (2008) Nanotechnology for site remediation. Remediat J 19(1):99–108. doi:10.1002/rem.20194

Pan B, Xing B (2012) Applications and implications of manufactured nanoparticles in soils: a review. Eur J Soil Sci 63(4):437–456. doi:10.1111/j.1365-2389.2012.01475.x

Phenrat T, Saleh N, Sirk K, Tilton RD, Lowry GV (2007) Aggregation and sedimentation of aqueous nanoscale zerovalent iron dispersions. Environ Sci Technol 41(1):284–290. doi:10.1021/Es061349a

Phenrat T, Saleh N, Sirk K, Kim H-J, Tilton R, Lowry G (2008) Stabilization of aqueous nanoscale zerovalent iron dispersions by anionic polyelectrolytes: adsorbed anionic polyelectrolyte layer properties and their effect on aggregation and sedimentation. J Nanopart Res 10(5):795–814. doi:10.1007/s11051-007-9315-6

Phenrat T, Cihan A, Kim H-J, Mital M, Illangasekare T, Lowry GV (2010) Transport and deposition of polymer-modified Fe^0 nanoparticles in 2-D heterogeneous porous media: effects of particle concentration, Fe^0 content, and coatings. Environ Sci Technol 44(23):9086–9093. doi:10.1021/es102398e

Ponder SM, Darab JG, Mallouk TE (2000) Remediation of Cr(VI) and Pb(II) aqueous solutions using supported, nanoscale zero-valent iron. Environ Sci Technol 34(12): 2564–2569. doi:10.1021/Es9911420

Reddi L, Ming X, Hajra M, Lee I (2000) Permeability reduction of soil filters due to physical clogging. J Geotech Geoenviron Eng 126(3):236–246. doi:10.1061/(ASCE)1090-0241(2000)126:3(236)

Rodgers JD, Bunce NJ (2001) Treatment methods for the remediation of nitroaromatic explosives. Water Res 35(9):2101–2111. doi:10.1016/s0043-1354(00)00505-4

Rojas TC, Sánchez-López JC, Greneche JM, Conde A, Fernández A (2004) Characterization of oxygen passivated iron nanoparticles and thermal evolution to γ-Fe_2O_3. J Mater Sci 39(15):4877–4885. doi:10.1023/B:JMSC.0000035328.99440.8d

Sakthivadivel R (1969) Clogging of a granular porous medium by sediment. Hydraulic Engineering Laboratory, College of Engineering, University of California, Berkeley

Saleh N, Sirk K, Liu YQ, Phenrat T, Dufour B, Matyjaszewski K, Tilton RD, Lowry GV (2007) Surface modifications enhance nanoiron transport and NAPL targeting in saturated porous media. Environ Eng Sci 24(1):45–57

Saleh N, Kim HJ, Phenrat T, Matyjaszewski K, Tilton RD, Lowry GV (2008) Ionic strength and composition affect the mobility of surface-modified Fe-0 nanoparticles in water-saturated sand columns. Environ Sci Technol 42(9):3349–3355. doi:10.1021/Es071936b

Schrick B, Hydutsky BW, Blough JL, Mallouk TE (2004) Delivery vehicles for zerovalent metal nanoparticles in soil and groundwater. Chem Mater 16(11):2187–2193. doi:10.1021/Cm0218108

Shi ZQ, Nurmi JT, Tratnyek PG (2011) Effects of nano zerovalent iron on oxidation-reduction potential. Environ Sci Technol 45(4):1586–1592

Simon JA (1997) Recent developments in cleanup technologies. Remediat J 8(1):129–136. doi:10.1002/rem.3440080113

Sun Y-P, X-q Li, Cao J, Zhang W-X, Wang HP (2006) Characterization of zero-valent iron nanoparticles. Adv Colloid

Interface Sci 120(1–3):47–56. doi:10.1016/j.cis.2006.03.001

Sun YP, Li XQ, Zhang WX, Wang HP (2007) A method for the preparation of stable dispersion of zero-valent iron nanoparticles. Colloid Surf A 308(1–3):60–66. doi:10.1016/j.colsurfa.2007.05.029

Tee YH, Bachas L, Bhattacharyya D (2009) Degradation of trichloroethylene and dichlorobiphenyls by iron-based bimetallic nanoparticles. J Phys Chem C 113(22):9454–9464. doi:10.1021/Jp809098z

Theron J, Walker JA, Cloete TE (2008) Nanotechnology and water treatment: applications and emerging opportunities. Crit Rev Microbiol 34(1):43–69. doi:10.1080/10408410701710442

Tratnyek PG, Johnson RL (2006) Nanotechnologies for environmental cleanup. Nano Today 1(2):44–48

Wang H, Kou X, Pei Z, Xiao J, Shan X, Xing B (2011) Physiological effects of magnetite (Fe_3O_4) nanoparticles on perennial ryegrass (*Lolium perenne* L.) and pumpkin (*Cucurbita mixta*) plants. Nanotoxicology 5(1):30–42. doi:10.3109/17435390.2010.489206

Wei Y-T, Wu S-C, Chou C-M, Che C-H, Tsai S-M, Lien H-L (2010) Influence of nanoscale zero-valent iron on geochemical properties of groundwater and vinyl chloride degradation: a field case study. Water Res 44(1):131–140. doi:10.1016/j.watres.2009.09.012

Wei Y-T, S-c Wu, Yang S-W, Che C-H, Lien H-L, Huang D-H (2012) Biodegradable surfactant stabilized nanoscale zero-valent iron for in situ treatment of vinyl chloride and 1,2-dichloroethane. J Hazard Mater 211–212:373–380. doi:10.1016/j.jhazmat.2011.11.018

Xi YF, Megharaj M, Naidu R (2011) Dispersion of zerovalent iron nanoparticles onto bentonites and use of these catalysts for orange II decolourisation. Appl Clay Sci 53(4):716–722. doi:10.1016/j.clay.2011.06.010

Yan W, Herzing AA, Kiely CJ, Zhang W-X (2010) Nanoscale zero-valent iron (nZVI): aspects of the core-shell structure and reactions with inorganic species in water. J Contam Hydrol 118(3–4):96–104. doi:10.1016/j.jconhyd.2010.09.003

Yan W, Vasic R, Frenkel AI, Koel BE (2012) Intraparticle reduction of arsenite (As(III)) by nanoscale zerovalent iron (nZVI) investigated with in situ X-ray absorption spectroscopy. Environ Sci Technol 46(13):7018–7026. doi:10.1021/es2039695

Zhang WX (2003) Nanoscale iron particles for environmental remediation: an overview. J Nanopart Res 5(3–4):323–332. doi:10.1023/A:1025520116015

Zhang W-X, Elliott DW (2006) Applications of iron nanoparticles for groundwater remediation. Remediat J 16(2):7–21. doi:10.1002/rem.20078

Zhang M, He F, Zhao DY, Hao XD (2011) Degradation of soil-sorbed trichloroethylene by stabilized zero valent iron nanoparticles: effects of sorption, surfactants, and natural organic matter. Water Res 45(7):2401–2414. doi:10.1016/j.watres.2011.01.028

Zhu X, Tian S, Cai Z (2012) Toxicity assessment of iron oxide nanoparticles in zebrafish (*Danio rerio*) early life stages. PLoS One 7(9):e46286. doi:10.1371/journal.pone.0046286